Block Copolymer Directed Nanoparticle for Fuel Cell Applications

Terry Dermis*, Sundar Mayavan*, Naba K. Dutta*, Namita Roy Choudhury* and Steven Holdcroft**

*Ian Wark Research Institute, ARC Special Research Centre, University of South Australia, Mawson Lakes Blvd., South Australia, Australia
**Department of Chemistry, Simon Fraser University, Canada

ABSTRACT

A simple method for synthesizing nanoparticles (NPs) using a fluorinated block copolymer is proposed. In this method, platinum NPs were introduced, via a reduction method, into a poly(vinylidene difluoride -*co*-hexafluoropropylene) -*b*- poly(methyl methacrylate) P((VDF-*co*-HFP)-*b*-PMMA) copolymer matrix. NP dispersion was characterized using transmission electron microscopy (TEM) coupled with an energy-dispersive x-ray (EDX) device for spectroscopic analysis, indicating whether NPs were selectively bound to one of the two phase separated copolymer blocks. Ultimately, exploitation of this technology would be a major advantage in the fuel cell market, specifically as the catalytic electrodes of proton exchange membrane fuel cells (PEMFCs).

Keywords: block copolymers, nanoparticles, self-assembly, fuel cell, AFM

1 INTRODUCTION

In recent years, researchers have attempted to develop various electrode structures for commercializing fuel cell systems. The crux of electrode performance would be the best electrocatalyst for a given charge transfer reaction. Platinum (Pt) alloys, and metal oxides have been the most effective electrocatalysts developed so far [1]. However, achieving high catalyst dispersion and subsequent improved access of the fuel towards it (i.e. high particle surface area), is a critical issue. This has led to intense research in developing a catalytic system in which metallic particles are directly deposited on to a block copolymer (BCP) matrix, enabling high dispersion of the catalytic particles whilst maintaining low Pt loadings. Generally, a block copolymer system containing dissimilar blocks A and B, is able to self-assemble into an ordered structure with a specific micro- or nano-domain orientation. The resulting BCP morphology and domain structure is directly related to the chemical nature of the blocks, molecular weight of each polymer block, the type of solvent and substrate used, and annealing times and temperatures [2]. In dilute solutions of selective solvents (i.e. selective to only one block), BCPs can intermolecularly associate to form aggregates. In such block copolymers, phase segregated polymer with formation of meso-domains with size ca. several tens of nanometers is observed. The situation is versatile and complicated since for a block copolymer system a solvent that is good for one block may be neutral, slightly selective, or strongly selective, depending on whether it is good, near Θ, or a non-solvent for the other block/s. The state of a system is principally governed by $\varphi\chi N$, where φ is the polymer volume fraction, χ is the interaction parameter between the individual component, and N is the total degree of polymerization. By controlling appropriately the segment nature and length of each constituent of the block in block copolymers, a wide variety of micro-domain structures of high degree of richness and complexity in solution phase are possible. Solution properties of block copolymers as well as their aggregation properties have long been investigated and have attracted much attention from both theoretical and experimental viewpoints. The knowledge of their solution behavior is of utmost importance for NP synthesis as they tend to act as nanoreactors by stabilizing the NPs within micelles of the diblock [3]. Control over the size and shape of the metal colloids can be achieved by 'growing' the desired colloids within domains of suitable size and shape. Block copolymers [4] and ionomers [5] comprising fluoro/non-fluoro segments have significant potential applications in the field of fuel cells. Recently, Shi and Holdcroft [6] successfully synthesized a series of high molecular weight block copolymers; P(VDF-*co*-HFP)-*b*-PMMA and P(VDF-*co*-HFP)-*b*-sulphonated PS (polystyrene). The former BCP was used in this study owing to the remarkable characteristics of PMMA and its viability in the proposed application. While a variety of procedures is found in the literature for synthesizing BCP nanocomposites, a convenient way of producing them is through the reduction of metal halides or anionic metal chloride precursors with alcohols, $NaBH_4$, Hydrazine or H_2 in the presence of BCP as a stabilizing agent [7]. Here we report the preparation and properties of these novel block copolymer nanocomposites for fuel cell catalyst applications. Pt based metallic precursors were incorporated into three compositions of block copolymer matrices and then reduced to metallic NPs within the BCP. The effect of copolymer composition and concentration on BCP self-organization, and NP deposition behavior, distribution, and size has been investigated using microscopic and spectroscopic techniques.

2 EXPERIMENTAL

2.1 Materials & Preparation

Poly(vinylidene difluoride-*co*-hexafluoropropylene)-*b*-poly(methyl methacrylate) (PVDF-*co*-HFP)-*b*-PMMA), synthesized at Simon Fraser University, Burnaby, Canada [6], was used as the model diblock copolymer without further ionization. Three samples of the copolymer were used possessing differing MMA molecular weights which contributed to dissimilar overall compositions for each of the samples (Table 1). Tetrahydrofuran (THF, reagent grade), was used as the selective solvent, where 0.1 wt%, 0.01 wt% and 0.005 wt% solutions were made from each of the samples. Pre-cleaned silicon wafers were used as substrates for applying thin films of the 0.01 and 0.005 wt% BCP/THF solutions, using a spin coater set at 4000 rpm.. These were then dried with high purity N_2 gas before being characterized using microscopic techniques.

The procedure for preparation of the BCP - stabilized colloid was as follows: $PtCl_4$ (Sigma Aldrich) (0.015 wt %) and P(VDF-*co*-HFP)-*b*-PMMA (0.1 wt %), were dissolved in THF and stirred overnight to form a pale yellow homogeneous solution. Sodium borohydride ($NaBH_4$) (Sigma Aldrich, ~1.5x the amount of $PtCl_4$ to assure complete reduction) was then added quickly with vigorous stirring. The color of the solution changed quickly from pale yellow to dark brown in a few seconds indicating that Pt(IV) ions were reduced to Pt^0 in aqueous solution. This dark brown solution was stirred overnight to give the BCP-stabilized metallic colloids. Each procedure was conducted under a N_2 atmosphere, where exposure to an open air atmosphere was kept to a minimum.

Table 1 : Molecular weight/compositions of each block in the three copolymer samples

Composition (%)	P(VDF-co-HFP) Mn^2 (g/mol)/PDI*	Block Mn^2 (g/mol)/PDI	PMMA Mn^3 (g/mol)
15/85	22k/1.50	147k/1.40	125k
65/35	22k/1.50	34k/1.41	12k
88/12	22k/1.50	25k/1.83	3k

*PDI = Polydispersivity Index

2.2 Characterization

BCP phase separation and morphology was analyzed by AFM using a NanoScope III Multimode SPM with controller from Digital Instruments, Veeco Metrology Group, Santa Barba, CA. All measurements were performed in tapping mode under ambient air using single-crystal silicon cantilevers. Data evaluation was performed with the NanoScope software version 5.30 (Digital Instruments, Veeco), and all images were flattened to the first order.

UV–Visible absorption spectra were recorded using a Varian Cary 1E UV/Vis spectrophotometer with a 10-mm quartz cell. The scanning range was from 200 to 800 nm. Baseline correction was made with respect to the THF solvent.

Transmission electron microscopy (TEM) was used to obtain micrographs of the Pt particles distributed among the block copolymer matrix, and possibly showing the resulting phase separated structure of each composition. A Philips CM200 operated at an accelerating voltage of 200kV and microscope fitted with an EDAX DX-4 energy-dispersive X-ray (EDX) system was used. A drop of dilute block copolymer/Pt^0 aqueous solution was dispensed onto carbon films supported by 200 mesh copper grids, where the solvent was allowed to evaporate before analysis took place.

3 RESULTS AND DISCUSSIONS

AFM analysis was conducted on the substrate cast diblock copolymer thin films. This technique was employed to examine confinement phenomena, such as the nanoscale patterns, formed due to the dissimilarity of the two block segments. Fluorinated and non-fluorinated polymer segments were expected to form highly ordered structures, dictated by the copolymer structure and molecular weights of each phase, substrate, film thickness, and selective solvent. Since the Si wafer is hydrophilic, it was expected that the PMMA segment would have a higher affinity for this surface in which it would reside to, whereas P(VDF-*co*-HFP), having a lower surface energy, would have a higher affinity for the free surface [8].

Figure 1 (a) shows definitive spherical type structures of one phase existing among the matrix of the other phase. The spheres are assigned to the P(VDF-*co*-HFP) phase, since the block ratio for this is of the lower order and, as in thin film geometries, the interfacial interactions impose restrictions on the local A-B segmental concentration profiles, hence, the lower surface energy of the fluorinated phase has caused these spheres to reside at the free surface. Annealing is expected to result in integration of like-segments, reducing the number of unfavorable A-B enthalpic contacts, in an attempt to decrease the overall free energy and the A-rich and B-rich domains may grow, in order to increase the surface to volume ratio. In an effort to maintain constant segmental density throughout this process, the copolymer chains must stretch beyond their equilibrium conformations. Also, due to the preferential interaction between the PMMA component and the Si substrate a higher degree of phase segregation of PMMA from the P(VDF-*co*-HFP) phase is probable, than if they were in the bulk.

The 65/35% composition, illustrated in Figure 1 (b), shows a unique phase separated structure of the two segments. Again, asymmetric equilibrium features evolve and due to molecular weight/compositional differences in the blocks, the system minimizes its free energy by creating

a discontinuous gyroid type structure. Here the P(VDF-*co*-HFP) phase is seen to construct this gyroidal network in a 'threaded-bead necklace' (TBN) type organization, where these bead-type domains seem to run along striations bringing about the complex gyroidal symmetry. This phase image is representative of a very dynamic system of which a level of ordering will result with time or under the influence of temperature.

Figure 1 (c) represents the 88/12% block copolymer composition. Here, the molecular weight of the P(VDF-*co*-HFP) is much higher than that of PMMA, resulting in the PMMA block forming small spherical domains aligned in a cross-hatch type ordered morphology. It is noticed that the smaller PMMA domains, where present, segregate the larger P(VDF-*co*-HFP) domains due to their affinity for the Si substrate. It is also observed that there is attachment of both P(VDF-*co*-HFP) and PMMA segments suggesting continuity, which is expected since corresponding blocks will segregate in an attempt to lower the overall free energy of the system.

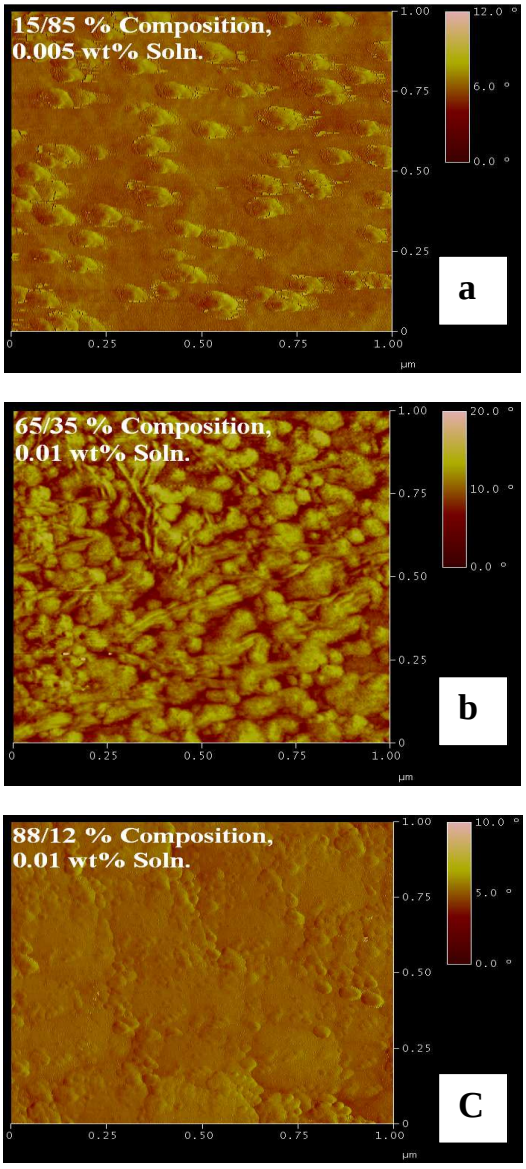

Figure 1 : (a), (b), and (c) represent 1 x 1 micron scanned AFM phase images of the various BCP systems cast on Si wafer substrates. Spherical domain diameters for each composition are: ~60-70 nm, ~40-60 nm, and ~25 – 45 nm (PMMA) and ~140 – 180 nm (P(VDF-co-HFP)) for the above images (a), (b), and (c), respectively.

All three images reveal that the copolymer exhibits a hierarchy of patterns, dependent on the BCP composition, and bulk solution concentration. The origin of pattern formation is thought to be associated with short-range and long-range van der Waals intermolecular forces [8].

The formation of P((VDF-*co*-HFP)-*b*-PMMA/Pt colloids via reduction of $PtCl_4$ with $NaBH_4$ was studied by UV-Vis spectroscopy. Once $NaBH_4$ was added to the mixture a new absorption band at 215 nm appeared and increased in intensity with time, which is characteristic of the colloidal Pt [9]. The resultant solution was mixed for 24 hrs in which UV/Vis results confirmed full reduction of $PtCl_4$ to Pt^0 after 24 hours (Figure 2).

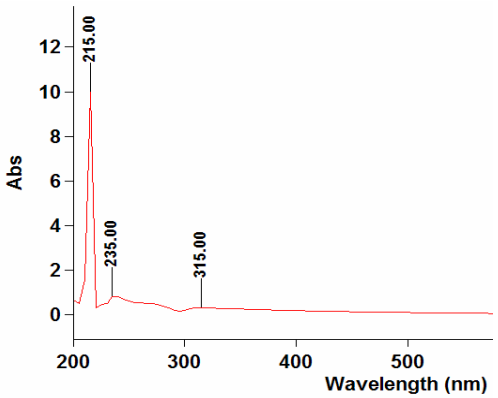

Figure 2 UV/Vis spectrum of Pt^0/15/85% BCP solution after 24 hrs mixing under N_2 atmosphere.

Figure 3 (a) and (b) show representative TEM images of the distribution of NPs within BCP nano-domains. If observed closely a contrast is seen along the contours where the Pt NPs are residing. This contrast mechanism in all TEM images possibly results from thickness and density fluctuations between the two phases. Low structural detail and poor contrast of the BCPs is accounted for due to the inability to stain either blocks with RuO_4 [10]. It is, however, observed that the metal particles are quite uniform and well distributed. This relates well with the assumption that the Pt colloids primarily reside to the hydrophilic PMMA phase and stabilization and association of Pt nanoparticles can be controlled by using this unique fluoro non-fluoro block copolymer. The average size of the Pt particles in all images (88/12 % composition not shown here) are about 2 – 3.5 nm in diameter which is much smaller than that of the commercial catalyst (dia ≈ 3.8 nm) [11]. We also conclude

that the NPs are stable amongst the BCP matrix since all TEM analysis was conducted 24 hours after full reduction had been confirmed by UV/Vis spectrophotometry measurements. It can be established from the weight percentages of the elements (shown in Table 2), detected by EDX analysis, that the Pt particles are residing to the PMMA phase since insignificant amounts of fluorine have been detected. Furthermore, silica was detected in all samples, and this can be accounted for from inevitable cross-contamination of all apparatus used. Hence, a well dispersed organization among the NPs, stabilized by the copolymer matrix, due to phase separation of the dissimilar blocks, can be seen.

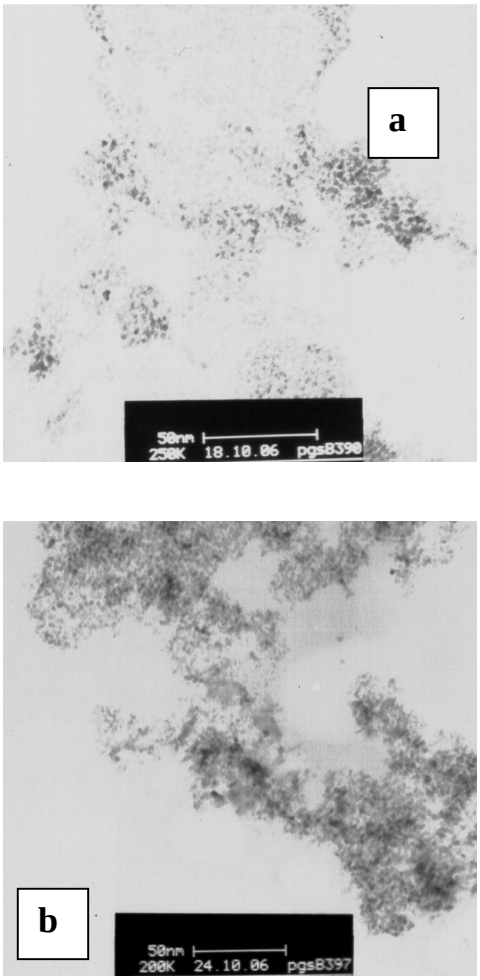

Figure **3**: Representative TEM images of (a) 15/85% and (b) 65/35% compositions with incorporated Pt nanoparticles. (Scale bar = 50 nm).

Table 2 : Weight percent distribution of elements found from TEM-EDX analysis for each composition. (Analysis performed on each TEM image shown in Figure 3).

Comp. (%)	C	O	F	Na	Si	Cl	Pt
15/85	40.5	5.8	0	3.2	3.4	0.7	46.4
65/35	17.3	0.9	0.3	0.2	1.9	0.2	79.2
88/12	32	2.2	0	0.2	1.8	0.4	63.5

4 CONCLUSION

AFM images indicated highly ordered BCP morphology with distinct patterns dependent on block compositions and copolymer concentration. TEM results demonstrate that stable, well dispersed nanocomposites can be achieved through selective incorporation of the NPs onto specific nano-domains of the phase-separated BCP. This method allows preparation of simple or complex highly ordered structured thin films with deposited NP arrays for use as electrocatalyst layers within a PEMFC membrane electrode assembly.

5 ACKNOWLEDGEMENTS

The authors wish to acknowledge the Australian Research Council for funding of this work through Discovery Grant. T. Dermis also gratefully acknowledges the funding provided by the Ian Wark Research Institute through an Honours scholarship.

6 REFERENCES

[1] A. H. Brian C. H. Steele *Nature* **2001**, *414*, 345.
[2] T. P. Lodge, *Macromolecular Chemistry and Physics* **2003**, *204*, 265-273.
[3] L. Zhang, H. Niu, Y. Chen, H. Liu and M. Gao, *Journal of Colloid and Interface Science* **2006**, *298*, 177-182.
[4] L. Rubatat, Z. Shi, O. Diat, S. Holdcroft and B. J. Frisken, *Macromolecules* **2006**, *39*, 720-730.
[5] R. A. Weiss, A. Sen, C. L. Willis and L. A. Pottick, *Polymer* **1991**, *32*, 1867-1874.
[6] Z. Shi and S. Holdcroft, *Macromolecules* **2004**, *37*, 2084-2089.
[7] R. M. R. H. Bönnemann, *Eur. J. Inorg. Chem* 2455-2480.
[8] P. F. Green and R. Limary, *Advances in Colloid and Interface Science* **2001**, *94*, 53-81.
[9] Z. Zhou, S. Wang, W. Zhou, L. Jiang, G. Wang, G. Sun, B. Zhou and Q. Xin, *Physical Chemistry Chemical Physics* **2003**, *5*, 5485-5488.
[10] J. S. Trent, J. I. Scheinbeim and P. R. Couchman, *Macromolecules* **1983**, *16*, 589-598.
[11] S. W. Zhenhua Zhou, Weijiang Zhou, Luhua Jiang, Guoxiong Wang, Gongquan Sun, Bing Zhou and Qin Xin, *Phys. Chem. Chem. Phys.*, **2003**, *5*, 5485 - 5488.